

NSLS-II STORAGE RING BPM BUTTON DEVELOPMENT*

A. Blednykh[#], B. Bacha, G. Bassi, W. Cheng, C. Hetzel, B. Kosciuk, D. Padrazo, O. Singh,
BNL, NSLS-II, Upton, NY, 11973-5000, USA

Abstract

The NSLS-II BPM Button design and its development process have been presented. Subjects discussed include BPM impedance optimization, design and construction, production, BPM selection and a first temperature measurement at 200mA average current within 1200 bunches.

IMPEDANCE OPTIMIZATION

Two types of BPM (beam position monitor) Buttons have been installed in the NSLS-II storage ring; the large aperture and the small aperture BPM Buttons. The large aperture BPM Button located on the multipole vacuum chambers of 12.5mm half-aperture, six BPMs per cell, 180 BPM assemblies total [1]. During the BPM Button optimization process we paid attention to: BPM Button heating due to trapped modes which are generated in the gap between the housing and the button [2]; heat transfer analysis; proper choice of the button and housing materials; dielectric materials choice from good thermal conductivity and low electrical conductivity point of views; impedance optimization process.

The large aperture BPM assemblies are located on the multipole vacuum chambers with antechamber slot of 10mm high. The standard BPM assembly consists of two BPM Flanges. Each BPM Flange, top and bottom, includes two BPM Buttons mounted into one flange as it shown in Fig. 1.

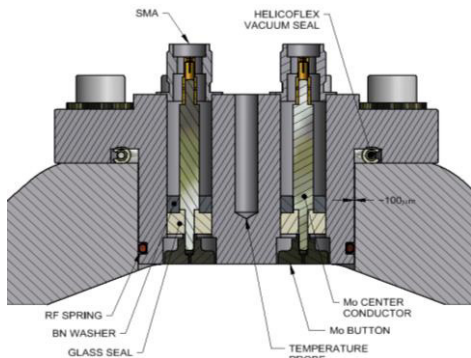


Figure 1: BPM Flange fixed to vacuum vessel. The clearance of the BPM Flange $\sim 100\mu\text{m}$ from the contact vacuum chamber surface.

The NSLS-II large aperture BPM button is chosen with a diameter of 7mm to satisfy horizontal and vertical BPM sensitivity requirements and to reduce heat load. It produces smaller geometric loss factor compared with a larger button diameter. The button thickness is chosen to be 2mm. The gap between the housing and the button is $250\mu\text{m}$. The BPM Button is made from molybdenum,

which has an electrical conductivity $\sigma_{Mo} = 17 \times 10^6 \text{ S/m}$ is much larger than the conductivity of stainless steel material chosen for the BPM Flange $\sigma_{Stst} = 1.5 \times 10^6 \text{ S/m}$. Due to different material selection, trapped mode power will be predominantly dissipated in the BPM Flange rather than in well-conducted button [3]. Due to excitation of resonant modes in the buttons, the kick factor and the loss factor depend very strongly on the BPM button geometry. Several types of modes can be generated in the button geometry by a passing bunch. A coaxial TEM-mode (signal) propagates through the button and the feedthrough to the BPM electronics. If the feedthrough is matched well to 50 Ohm, there will be no TEM-modes reflected back to the chamber. Coaxial cavity type modes TE_{m1p} -mode (H_{m1p} -mode) where m and p are 1, 2, 3, k (field variation in azimuthal and longitudinal directions). These modes then can be seen by the beam at frequencies defined by the cut-off frequency. The cut-off frequency for H_{m1} -mode like in a coaxial waveguide can be defined as

$$f_c^{H_{m1}} \approx \frac{1}{\sqrt{\epsilon_r}} \frac{c}{\pi} \frac{m}{(r_1+r_2)}, \quad (1)$$

Where r_1 and r_2 are the radii of the inner and outer conductors, $m=1, 2, 3, k$ and ϵ_r is relative permittivity (dielectric constant). As can be seen from Fig. 2, there are two types of dielectric materials present in the button geometry. It is 7070 glass (SiO_2) for the vacuum seal and a Boron Nitride (BN) disc installed on the ambient side of the glass seal to improve the heat transfer from the pin to the stainless flange.

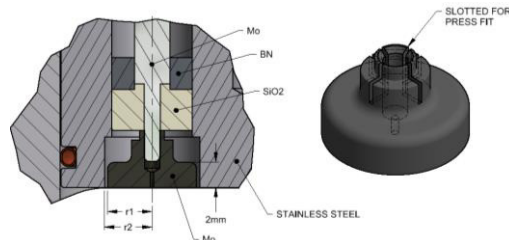


Figure 2: Internal button details with press fit connection.

The longitudinal wake potential for a 3mm Gaussian bunch and its Fast Fourier Transform are shown in Figs. 3,4. For the numerical calculation “port” boundary condition was specified at the end of the button. In this case the TEM-mode propagates out of the button without reflection. The first lowest mode is H_{11} -Mode (TE_{11} -mode). It is trapped in a gap between the housing and the button due to the button shape at frequency $f_{H11} = 13.4\text{GHz}$, which is slightly above the cut-off frequency $f_c^{H11} = 13.2\text{GHz}$ ($r_1 = 3.5\text{mm}$ and $r_2 = 3.75\text{mm}$). The peak at frequency 25.95GHz corresponds to the same type of mode with $m = 2$ (H_{21} -Mode). Two other peaks were identified at frequencies 15.43GHz and

* Work supported by DOE contract DE-SC0012704.
#blednykh@bnl.gov

24.4GHz due to dielectric materials (BN and SiO₂) located above the BPM Button (Fig.2) and its field radiates in to the beam channel. Since the bunch length during operation at 500mA average current expected to be 9mm with installed Landau cavity and three damping wigglers, no HOM will be generated and seen by the beam.

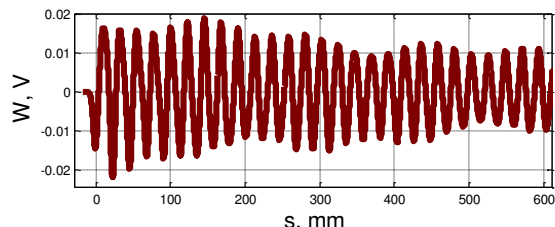


Figure 3: Longitudinal long-range wakepotential.

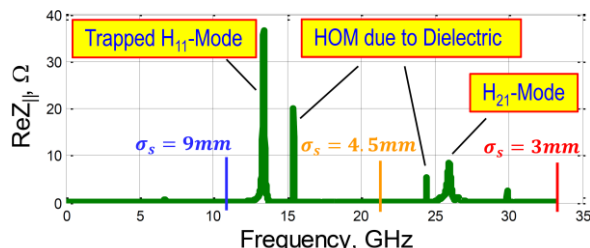


Figure 4: Real part of the longitudinal impedance.

To avoid generation of HOM's due to $\sim 100\mu\text{m}$ clearance gap between the BPM Flange and the vacuum chamber (Fig. 5), RF Spring was installed into machined groove (Figs. 1,2) at a height of 1.5mm from the surface edge. In Fig. 6 the longitudinal impedance is presented for the BPM Flange geometry with and without RF Spring.

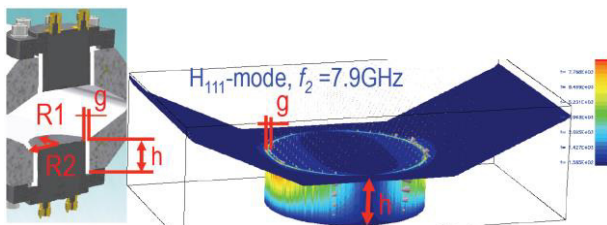


Figure 5: The BPM Flange model with $\sim 100\mu\text{m}$ clearance from the contact vacuum chamber surface.

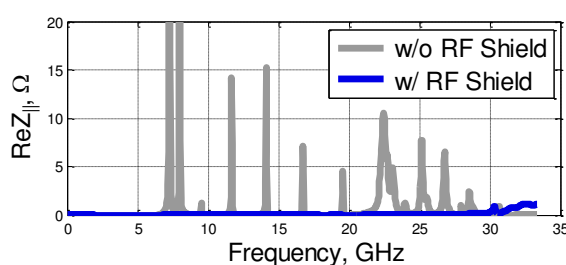


Figure 6: Real Part of the Longitudinal Impedance.

DESIGN AND CONSTRUCTION

Sensitivity calculations revealed that an optimal button configuration for the 25mm vertical aperture of the NSLS-II vacuum chamber was a 7mm diameter button

5: Beam Dynamics and EM Fields

D04 - Beam Coupling Impedance - Theory, Simulations, Measurements, Code Developments

with 16mm center to center button spacing. With such a small space between buttons, a dual button design was chosen where two feedthroughs were installed in a common flange (Fig. 1). This design had the added benefit of simplifying installation and reducing the number of vacuum seals by a factor of two. A Helicoflex Delta seal was chosen as a UHV seal. This placed stringent requirements on the surfaces finish of both the BPM flange and the vacuum chamber sealing surfaces. The vendor specified a 16 micro-inch finish with a circular lay. During production of the 515 units that were procured for NSLS-II, this feature proved to be challenging to achieve and resulted in a fairly large number of rejects. An important design consideration was to ensure that there was an adequate thermal path for any trapped mode heat generation. Electromagnetic simulations showed as much as 1 watts per button (at 500mA) and since the vendor chose doped 7070 glass for the vacuum seal which has an extremely low thermal conductivity, it was decided that a Boron Nitride disc installed on the ambient side of the glass seal would be an effective path to sink any heat into the stainless flange and ultimately the aluminium vacuum chamber.

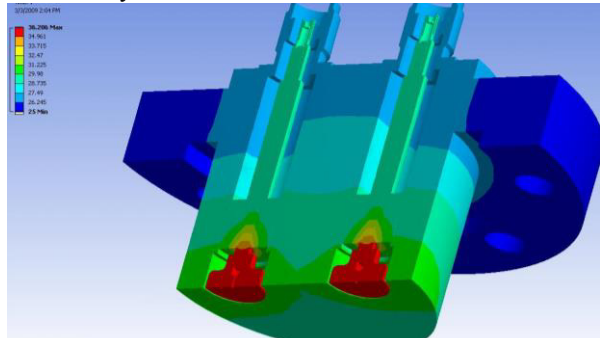


Figure 7: Thermal analysis of the NSLS-II BPM Flange. Temperature distribution of 7070 glass insulator backed with Boron Nitride washer. 1 Watt applied to each button.

PRODUCTION

A contract was awarded to Times Microwave to produce 515 dual button BPM assemblies for NSLS-II. Five first article units were manufactured and tested at BNL. Testing included capacitance measurement, geometric inspection, leak testing, vacuum seal surface inspection and SMA connector insertion force. Afterwards, production units arrived in larger quantities and it was decided to perform electrical, geometric and vacuum acceptance testing on 100% of the units received. Of the 515 ordered, 21 units were rejected primarily due to vacuum issues or failed dimensional inspection. A problem was also later discovered where the buttons which were pressed on during assembly would fall off during installation in the vacuum chambers. Post mortem inspection revealed this failure was due to poor quality control during the manufacture and inspection of the molybdenum buttons and center conductors. This resulted in the rejection of several units.

BPM BUTTON SELECTION

RF BPM button is a wideband vacuum sealed coaxial feedthrough. It's used to detect and measure the beam electromagnetic field, and to inject signals to the beam when needed (kick, or damp the beam). Because it has only one RF port, the most important parameter is S11 in frequency domain. The reflected waveform can be displayed in VSWR and reflection coefficient format.

Another common way for evaluating the feedthrough transmission line is the time domain reflectometry: A fast edge pulse is launched into the button transmission line by a step generator. The incident and reflected voltage waves are monitored by an oscilloscope; the response will show position and nature of the discontinuities (resistive, inductive, or capacitive) along the line, see Fig.8. Time domain was used as a verification and troubleshooting tool.

Appropriate measurement and calibration techniques, along with appropriate instruments configured for this test purpose were used. BPM capacitance was calculated for specified geometric Button dimensions as a reference value for further comparison with measured data.

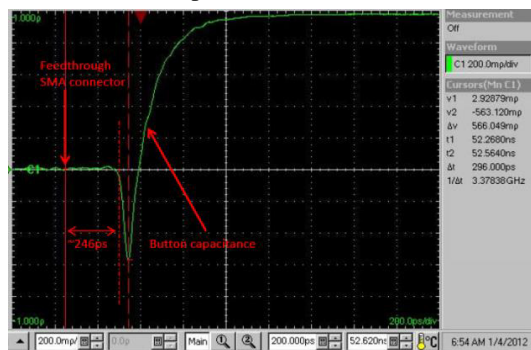


Figure 8: BPM button TDR measurement with DSA8200 and 80E04 sampling module. Feedthrough transmission line length is $256/2\text{ps} = 123\text{ps}$

The Button capacitance has been measured using a VNA S11 in Smith chart format. Two-port calibration must be performed prior making measurement, for a one-port calibration use port extension on port to which the button is connected; extension length is the transmission line length (as in Fig.9). Forward reflection S11 in smith chart format is measured. Z_0 can be viewed as the impedance of the source, and Z_L is the button impedance. The reflection coefficient is completely defined by the impedance Z_L and the reference impedance Z_0 (50Ω). The complex reflection coefficient is given by: $\Gamma = \frac{Z_L - Z_0}{Z_L + Z_0}$. Measured capacitance deviation between the two assemblies is 0.94%. The capacitance value is calculated by integrating and scaling the reflected waveform [4] for data comparison.

CONCLUSION

Two large aperture BPM Button assemblies in C2 and C4 straight sections were installed with several RTD

(resistance temperature detectors) temperature sensors to monitor temperature rise. Two RTDs are installed very close to the BPM Buttons inside of the top and the bottom BPM Flange as it shown in Fig. 1. Two RTDs are mounted outside, on SMA connectors, on the chamber surface and on BPM flange surface. In Fig. 10 we plot the temperature rise as a function of time. The blue shaded area reflects the average current increase up to 200mA.

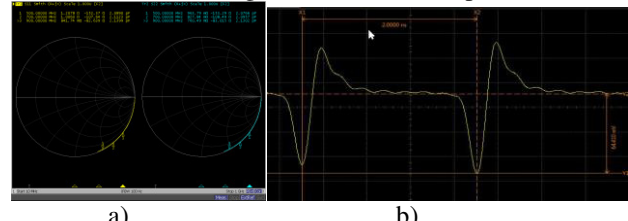


Figure 9: Large aperture BPM Button dual assembly capacitance measurement example (a). Large aperture BPM Button signal captured on a 4GHz scope (b).

The internal temperature of the BPM Flange (RTD named “top BPM internal” and “bottom BPM internal” rise to $26.5\text{ }^{\circ}\text{C}$. The temperature difference is $1.3\text{ }^{\circ}\text{C}$. The predicted BPM temperature distribution shown is Fig 7 was based on 1 watt applied to each button corresponding to 500 mA beam current and shows a temperature rise of $5\text{ }^{\circ}\text{C}$ in the area of the RTD probe. If this simulation were run for 200 mA with 0.4 watts applied to each button, we can expect a $2\text{ }^{\circ}\text{C}$. More comprehensive studies will be done in near future on temperature dependence as a function of bunch length and the number of bunches.

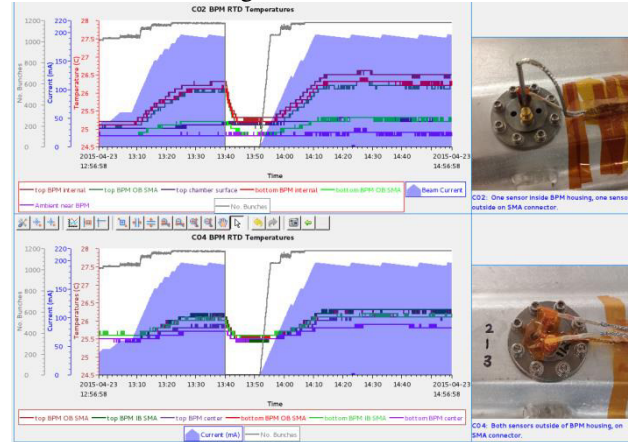


Figure 10: Temperature rise measurements. The average current 200mA was achieved within $M=1200$ bunches.

REFERENCES

- [1] O. Singh et al., “NSLS-II Beam Diagnostics Overview”, PAC09, Vancouver, Canada, May 2009.
- [2] C.-K. Ng et al., “Simulation of PEP-II Beam Position Monitors”, SLAC-PUB-95-6899, May 1995.
- [3] I. Pinayev and A. Blednykh, “Evaluation of Heat Dissipation in the BPM Buttons”, PAC09, Vancouver, Canada, May 2009.
- [4] W. Cheng et al., “Performance of NSLS2 Button BPM’s”, Proceedings of IBIC2013, Oxford, UK.

5: Beam Dynamics and EM Fields